

# NAVAL POSTGRADUATE SCHOOL

## Monterey, California



### THESIS

#### AN ANALYSIS OF A SATELLITE SURVEILLANCE SYSTEM

by

Sarawoot Chiyangabut

March 1999

Thesis Advisors:  
Second Reader:

J.N. Eagle  
Supachai Sirayanone

Approved for public release; distribution is unlimited.

19990504 076

{PRIVATE }{PRIVATE } <b>REPORT</b> <b>DOCUMENTATION PAGE</b>			Form Approved OMB No. 0704-0188	
Public reporting burden for this collection of information is estimated to average 1 hour per response, including the time for reviewing instruction, searching existing data sources, gathering and maintaining the data needed, and completing and reviewing the collection of information. Send comments regarding this burden estimate or any other aspect of this collection of information, including suggestions for reducing this burden, to Washington headquarters Services, Directorate for Information Operations and Reports, 1215 Jefferson Davis Highway, Suite 1204, Arlington, VA 22202-4302, and to the Office of Management and Budget, Paperwork Reduction Project (0704-0188) Washington DC 20503.				
1. AGENCY USE ONLY (Leave blank)		2. REPORT DATE March 1999		3. REPORT TYPE AND DATES COVERED Master's Thesis
4. TITLE AND SUBTITLE : AN ANALYSIS OF A SATELLITE SURVEILLANCE SYSTEM				5. FUNDING NUMBERS
6. AUTHOR(S) Sarawoot Chiyangabut				
7. PERFORMING ORGANIZATION NAME(S) AND ADDRESS(ES) Naval Postgraduate School Monterey, CA 93943-5000				8. PERFORMING ORGANIZATION REPORT NUMBER
9. SPONSORING / MONITORING AGENCY NAME(S) AND ADDRESS(ES) N/A				10. SPONSORING / MONITORING AGENCY REPORT NUMBER
11. SUPPLEMENTARY NOTES The views expressed in this thesis are those of the author and do not reflect the official policy or position of the Department of Defense or the U.S. Government.				
12a. DISTRIBUTION / AVAILABILITY STATEMENT Approved for public release; distribution is unlimited.				12b. DISTRIBUTION CODE
13. ABSTRACT (maximum 200 words) A new procedure is proposed to evaluate the effectiveness of surveillance satellites in circular orbits. It is assumed that the times of target detections by the satellite are given by a nonhomogeneous Poisson process with detection rate at time $t$ of $\rho(t) = f(\lambda(t), \beta_1(t), \beta_2(t))$ , where $\lambda(t)$ is the angular distance between the target and subsatellite point, $\beta_1(t)$ is great circle bearing from the target to the subsatellite point, and $\beta_2(t)$ is great circle relative bearing from the subsatellite point to the target. In some circumstances, the dependence of $\rho(t)$ on $\beta_1(t)$ and $\beta_2(t)$ can be ignored, making $\rho(t)$ only a function of $\lambda(t)$ . Then the probability of target detection on a single satellite pass becomes a function of only the minimum angular distance, or lateral range, between the target and subsatellite point. A numerical method using Newton's method is developed for computing the local minimum of $\lambda(t)$ . Probabilities of detection using this procedure are compared to those computed with existing methods of Wertz and Washburn.				
14. SUBJECT TERMS Surveillance Satellite, Lateral Range Curve, Angular Distance, Probability of Detection, Poisson Process				15. NUMBER OF PAGES 74
				16. PRICE CODE
17. SECURITY CLASSIFICATION OF REPORT Unclassified		18. SECURITY CLASSIFICATION OF THIS PAGE Unclassified		19. SECURITY CLASSIFICATION OF ABSTRACT Unclassified
				20. LIMITATION OF ABSTRACT UL

NSN 7540-01-280-5500

Standard Form 298 (Rev. 2-89)  
Prescribed by ANSI Std. Z39-18



Approved for public release; distribution is unlimited

## AN ANALYSIS OF A SATELLITE SURVEILLANCE SYSTEM

Sarawoot Chiyangcabut  
Lieutenant, Royal Thai Navy  
B.S., Royal Thai Naval Academy, 1991

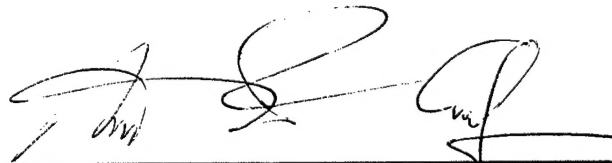
Submitted in partial fulfillment of the  
requirements for the degree of

## MASTER OF SCIENCE IN OPERATIONS RESEARCH

from the

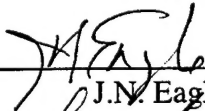
NAVAL POSTGRADUATE SCHOOL  
March 1999

Author:



Sarawoot Chiyangcabut

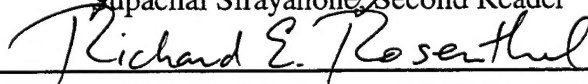
Approved by:



J.N. Eagle, Thesis Advisor



Supachai Sirayanone, Second Reader



Richard E. Rosenthal, Chairman  
Department of Operations research



## ABSTRACT

A new procedure is proposed to evaluate the effectiveness of surveillance satellites in circular orbits. It is assumed that the times of target detections by a satellite are given by a nonhomogeneous Poisson process with detection rate at time  $t$  of  $\rho(t) = f(\lambda(t), \beta_1(t), \beta_2(t))$ , where  $\lambda(t)$  is the angular distance between the target and subsatellite point,  $\beta_1(t)$  is great circle bearing from the target to the subsatellite point, and  $\beta_2(t)$  is great circle relative bearing from the subsatellite point to the target. In some circumstances, the dependence of  $\rho(t)$  on  $\beta_1(t)$  and  $\beta_2(t)$  can be ignored, making  $\rho(t)$  only a function of  $\lambda(t)$ . Then the probability of target detection on a single satellite pass becomes a function of only the minimum angular distance, or lateral range, between the target and subsatellite point. A numerical method using Newton's method is developed for computing the local minima of  $\lambda(t)$ . Probabilities of detection using this procedure are compared to those computed with existing methods of Wertz and Washburn.



## TABLE OF CONTENTS

I. INTRODUCTION.....	1
II. BACKGROUND THEORIES .....	3
A. SATELLITE ORBIT .....	3
1. Reference System .....	3
2. Laws of Motion .....	3
3. Orbit Types.....	6
a. Elliptical Orbit .....	6
(1) Geometry of an Elliptical Orbit.....	6
(2) Elements of an Elliptical Orbit.....	8
b. Circular Orbit.....	9
4. Satellite Ground Track.....	11
B. ORBITAL COVERAGE.....	12
1. Target Elevation Constraint.....	12
2. Horizon Constraint .....	12
C. FRACTION OF COVERAGE EQUATIONS .....	13
1. Wertz's Equations.....	13
2. Washburn's Equation.....	15
III. MODEL DEVELOPMENT.....	17
A. GENERAL ASSUMPTIONS FOR MATHEMATICAL MODEL DEVELOPMENT .....	17
B. DETECTION PARAMETERS.....	18
1. Angular Distance .....	18
2. Target Azimuth Angle .....	21
3. Sensor Azimuth Angle.....	22
C. PROBABILITY OF DETECTION.....	23



D. MINIMUM VALUE OF ANGULAR DISTANCE .....	24
IV. EXPERIMENTATION AND RESULT .....	29
A. EXPERIMENTATION .....	29
B. RESULTS .....	32
C. DISCUSSION OF RESULTS .....	34
V. CONCLUSIONS .....	37
A. CONCLUSIONS .....	37
B. SUGGESTION FOR FURTHER STUDIES .....	37
APPENDIX A. SPHERICAL GEOMETRY FORMULAS .....	39
APPENDIX B. FORMULATION OF TARGET AZIMUTH ANGLE .....	43
APPENDIX C. FORMULATION OF SENSOR AZIMUTH ANGLE .....	45
APPENDIX D. FIRST AND SECOND DERIVATIVES .....	47
APPENDIX E. MINIMUM VALUES OF ANGULAR DISTANCE .....	49
LIST OF REFERENCES .....	55
INITIAL DISTRIBUTION LIST .....	57

## LIST OF FIGURES

Figure 2.1 Geocentric Coordinate System.....	4
Figure 2.2 Orbit Geometry .....	7
Figure 2.3 Classical Orbital Elements.....	8
Figure 2.4 Circular Orbit .....	10
Figure 2.5 Determination of Subsatellite Point.....	11
Figure 2.6 Coverage Angular Radius .....	13
Figure 2.7 Regions of Coverage.....	14
Figure 3.1 Detection Parameters .....	19
Figure 3.2 Angular Distance and Anomaly .....	20
Figure 3.3 Determination of Target Azimuth Angle .....	21
Figure 3.4 Determination of Sensor Azimuth Angle .....	23
Figure 3.5 Angular Distance against Anomaly .....	27
Figure 3.6 Probability of Detection versus Time .....	28
Figure 3.7 Cumulative Probability of Detection versus Time.....	28
Figure 4.1 Lateral Range Curve .....	31



## LIST OF TABLES

Table 3.1. Closest Point of Approach and Probability of Detection .....	27
Table 4.1. Average Probability of Detection .....	33
Table E-1. Target's Latitude at 0° .....	49
Table E-2. Target's Latitude at 15° .....	50
Table E-3. Target's Latitude at 30° .....	50
Table E-4. Target's Latitude at 50° .....	51
Table E-5. Target's Latitude at 55° .....	51
Table E-6. Target's Latitude at 64° .....	52
Table E-7. Target's Latitude at 65° .....	52
Table E-8. Target's Latitude at 70° .....	53
Table E-9. Target's Latitude at 75° .....	53
Table E-10. Target's Latitude at 80° .....	54



## EXECUTIVE SUMMARY

Earth orbiting artificial satellites play a significant role in surveillance missions. To help evaluate surveillance satellite performance, it is important to find an appropriate measure of effectiveness (MOE). A reasonable MOE for surveillance missions is probability of detection.

This thesis assumes that the times of target detection by a satellite are given by a nonhomogeneous Poisson process with rate at time  $t$  of  $\rho(t) = f(\lambda(t), \beta_1(t), \beta_2(t))$ , where  $\lambda(t)$  is the angular distance between the target and subsatellite point,  $\beta_1(t)$  is the great circle bearing from the target to the subsatellite point, and  $\beta_2(t)$  is the great circle relative bearing from the subsatellite point to the target. Professor Alan R. Washburn at the Naval Postgraduate School gives an expression for  $\lambda(t)$ . Formulas for the azimuth angles  $\beta_1(t)$  and  $\beta_2(t)$  are given here.

If the dependence of detection rate on  $\beta_1$  and  $\beta_2$  is not strong, then it is possible to express the probability of detection on a single pass as a function of the minimum angular separation (or lateral range) between the target and subsatellite point. A numerical procedure using Newton's method is developed to compute the local minima of  $\lambda(t)$  for use in this model.

Four analytical models for estimating the probability of detection have been tested. Two are lateral range curve models using the methods of this thesis; the third is a well-known Earth coverage model; and the fourth is a detection model by Washburn. The numerical results show that the newly developed methods yield probabilities of detection

comparable to the existing models. The advantage of the new methods presented here is that they allow more specific modeling of the target position, environmental conditions and sensor types.

## ACKNOWLEDGMENT

Special thanks are given to the Royal Thai Navy for giving me the scholarship to study in the United States. I would like to express my sincere appreciation to my thesis advisor, Professor J.N. Eagle, for his understanding, indispensable assistance and guidance in the completion of this thesis. I would like to gratefully acknowledge my second reader, Professor Supachai Sirayanone, as we have spent quite a number of day and night hours working on the draft of this thesis.

I also would like to thank Professor Alan R. Washburn, Professor Siriphong Lawphongpanich, and Professor D.A. Danielson for their help and recommendations.





## I. INTRODUCTION

Earth orbiting artificial satellites have been developed to perform a wide variety of military missions, including early warning, attack assessment, navigation, communications, meteorology, geodesy, surveillance and reconnaissance (Friedman et al., 1985). As reliance on military satellites has grown, so has the importance of achieving the best possible performance subject to resource and environmental constraints. Appropriate measures of effectiveness (MOE) will vary with different mission types, but for search and detection missions, a reasonable MOE is probability of detection.

There are many possible methods for using probability of detection as a satellite search MOE. Perhaps the simplest approach is to compute the fraction of a specified latitude line that is "covered" by one satellite orbit with a specified swath width (Wertz, 1992). This method generally assumes a non-rotating Earth, but is nonetheless well suited for satellites in low Earth orbit, a common orbit for military applications.

Washburn proposed a satellite model which takes the Earth's rotation into account. As a satellite moves from its southernmost latitude to northernmost latitude (a "pass"), the swath width will include a certain fraction  $g$  of the latitude line passing through a target. Washburn's equations determine this fraction  $g$ , but require that the swath width of the satellite pass be small (Washburn, 1997).

This thesis work is intended to develop a new mathematical formulation to improve on the Wertz and Washburn models. Our preliminary work will be to examine both procedures. The new method will assume that times of target detection are given by

a nonhomogeneous Poisson process with rate at time  $t$  of  $\rho(t) = f(\lambda(t), \beta_1(t), \beta_2(t))$ , where  $\lambda(t)$  is the angular distance between the target and subsatellite point,  $\beta_1(t)$  is the great circle bearing from the target to the subsatellite point, and  $\beta_2(t)$  is the great circle relative bearing from the subsatellite point to the target. When dependence on  $\beta_1$  and  $\beta_2$  is not strong, then detection rate can be express as a function of only  $\lambda(t)$ . In these cases, the probability of detection during a single pass can be expressed as a function of the minimum angular distance between the target and subsatellite point. We will develop a numerical procedure to compute local minima of  $\lambda(t)$  for use in the lateral range curve models.

The foundations of satellite orbital mechanics are introduced in Chapter II, BACKGROUND THEORIES. Chapter III, MODEL DEVELOPMENT, details the crucial parameters affecting the satellite's detection rate. The method of determining the minimum value of angular distance is also discussed. Four analytical models for estimating the probability of detection of a target by a surveillance satellite are tested and compared in Chapter IV, EXPERIMENTATION AND RESULTS. Finally, Chapter V, CONCLUSIONS, summarizes the models being developed, draws conclusions and suggests areas of further research.

## **II. BACKGROUND THEORIES**

This chapter provides the basics of Earth satellite orbital mechanics and discusses Wertz's and Washburn's probability of detection models.

### **A. SATELLITE ORBIT**

#### **1. Reference System**

In dealing satellite orbits, it is important to select an appropriate coordinate system. If the correct coordinate system is selected, the development of equations of motion can be simple. Of the many possible coordinate systems, we will use a geocentric coordinate system fixed in inertial space.

In this coordinate system, the equatorial plane is used as a primary plane, and the meridian passing through Greenwich, called a prime meridian, is used as a secondary plane. The origin of the system is the center of the Earth. A position in this coordinate system is determined by latitude ( $\psi$ ), and longitude ( $L$ ), defined in the usual way and illustrated in Figure 2.1.

#### **2. Laws of Motion**

In order to understand and predict satellite motion, it is necessary to know the basic laws defining satellite motion. The most well-known laws are Kepler's Laws, Newton's Law of Motion, and Newton's Universal Law of Gravitation.

Johann Kepler (1571-1630) empirically discovered three laws of planetary motion by studying the detailed observational record of Tycho Brahe (Vallado, 1997). They are:

First law: The orbit of each planet is an ellipse, with the Sun at one focus.

Second law: The line joining the planet to the Sun sweeps out equal areas in equal times.

Third law: The square of the period of a planet is proportional to the cube of its mean distance from the Sun.

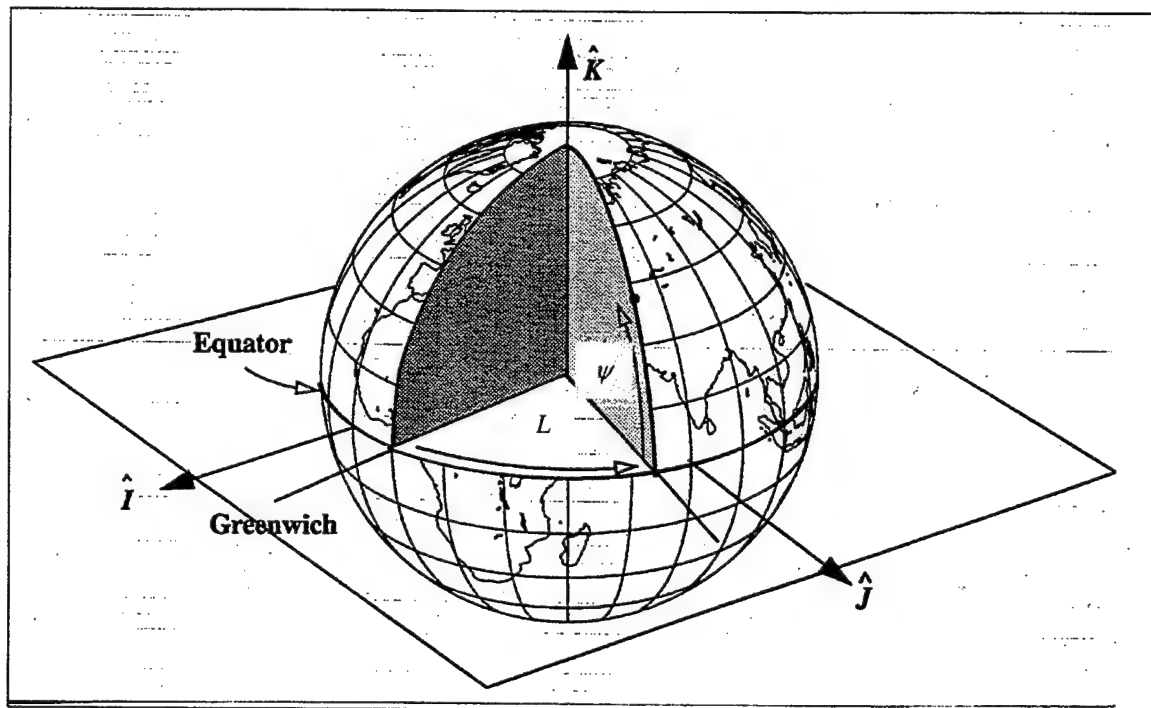


Figure 2.1 Geocentric Coordinate System (Vallado, 1997)

The laws apply to a satellite revolving around the Earth as well as planets revolving around the Sun.

Kepler's Laws did not completely solve the planetary motion problem. Isaac Newton (1642-1727) introduced his additional three laws of motion to help solve problems about the dynamics of motion (Vallado, 1997). They are:

First law: A body continues in its state of rest, or of uniform motion in a straight line, unless compelled to change that state by forces impressed upon it.

Second law: The change of motion is proportional to the motive force impressed and is made in the direction of the right line in which that force is impressed.

Third law: To every action there is always opposed an equal reaction or, the mutual actions of two bodies upon each other are always equal and directed to contrary parts.

The motions of satellites and planets are primarily driven by gravitation. Newton formulated the Universal Law of Gravitation to describe gravitational force between two bodies. Newton's Universal Law of Gravitation states that the force of gravity between two celestial bodies is directly proportional to the product of their two masses and inversely proportional to the square of the distance between them. Symbolically,

$$F_g = \frac{Gm_1m_2}{R^2}, \quad (2-1)$$

where

$F_g$  = gravitational force in Newtons (N),

$G$  = universal gravitation constant =  $6.67 \times 10^{-11} \text{ N} \times \text{m}^2/\text{kg}^2$ ,

$m_1, m_2$  = mass of two bodies (kg), and

$R$  = distance between the two bodies (m).

One of Newton's achievements was to show that Kepler's Laws follow from Newton's Laws of Motion and Universal Gravitation.

### 3. Orbit Types

As Kepler did, we will assume here that all satellite orbits are elliptical or as a special case, circular. "Keplerian" orbits ignore the gravitational effects of the Earth's equatorial bulge and atmospheric drag.

#### a. *Elliptical Orbit*

(1) *Geometry of an Elliptical Orbit* Figure 2.2 illustrates the geometry of an elliptical satellite orbit. It has two distinct foci. One is called the primary focus and coincides with the center of the Earth. The semi-major and semi-minor axes are  $a$  and  $b$ , respectively. Half the distance between the two foci is  $c$ . The farthest point and the nearest point from Earth in an elliptical satellite orbit are called apogee and perigee, respectively.  $R_a$  is the radius of an apogee, the maximum distance between the Earth's center and the satellite. And the minimum distance  $R_p$  is the radius of a perigee.  $\bar{R}$  is a satellite position vector relative to the center of the Earth.  $\bar{V}$  is a satellite velocity vector relative to the center of the Earth. The flight-path angle ( $\phi$ ) is the angle between the velocity vector and a line perpendicular to a satellite position vector  $\bar{R}$ . The true anomaly,  $\theta$ , locates a satellite's position in the orbital plane. It is measured from the perigee to a satellite position vector  $\bar{R}$  in the direction of satellite motion.

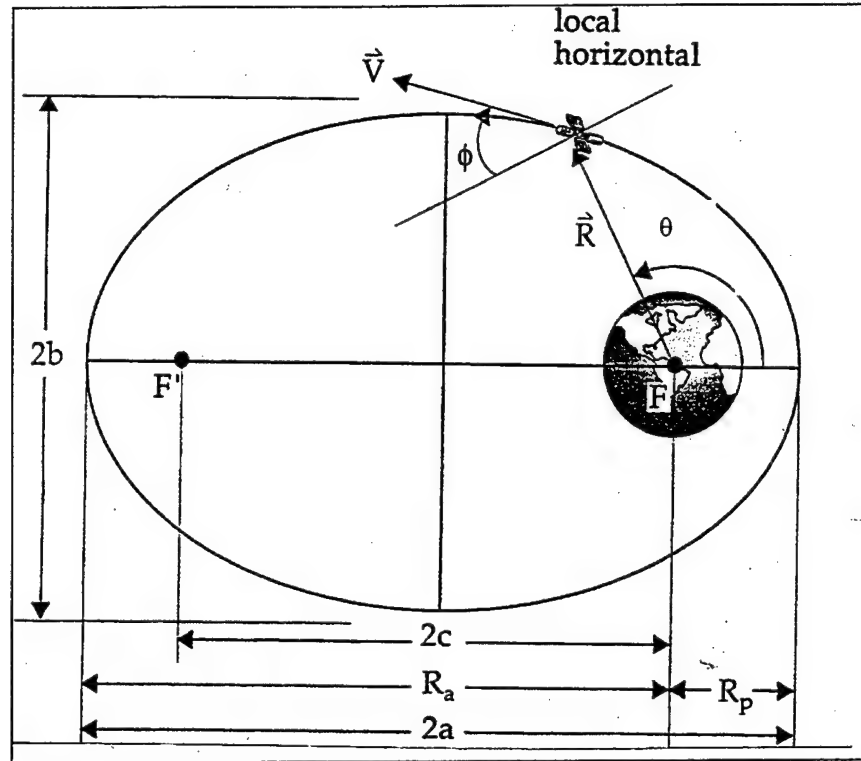


Figure 2.2 Orbit Geometry (Larson & Wertz, 1992)

The motion of a satellite orbiting the Earth can be represented as the polar equation of a conic section.

$$R = \frac{a(1 - e^2)}{1 + e \cos \theta} \quad (2-2)$$

where  $R$  = magnitude of the position vector  $\vec{R}$ ,

$a$  = semi-major axis (km),

$e$  = eccentricity, given by  $e = \frac{c}{a}$ , and

$\theta$  = true anomaly or the polar angle.

This equation is appropriate for both circular ( $e=0$ ) and elliptical ( $0 < e < 1$ ) orbits.



(2) *Elements of an Elliptical Orbit* Six classical orbital elements are required to specify a satellite orbit and the satellite position on that orbit. These elements allow us to visualize orbital size, shape, and orientation. Figure 2.3 illustrates the six classical orbital elements.

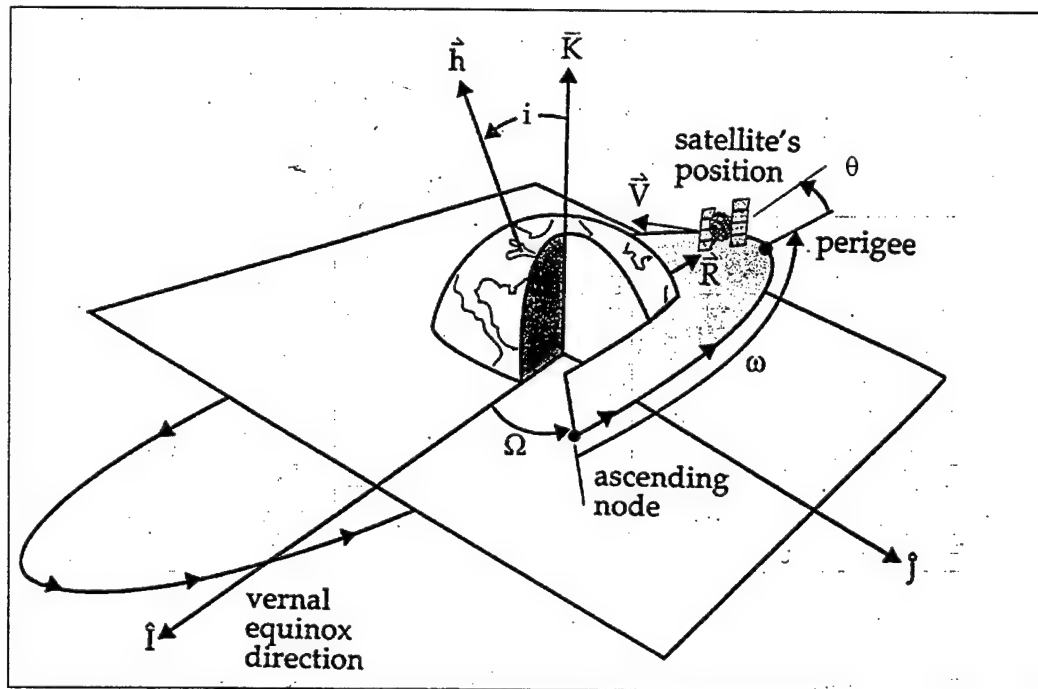


Figure 2.3 Classical Orbital Elements (Sellers, 1994)

The semi-major axis,  $a$ , has already been discussed. The second element is the eccentricity,  $e$ . It describes the shape of orbit, and is computed as  $e = \frac{c}{a}$ . For closed orbits,  $0 \leq e < 1$ . The circular orbit has an eccentricity of 0. The inclination  $i$  is the angle between the equatorial and orbital planes. The right ascension of ascending node ( $\Omega$ ) (or a longitude of the ascending node) is the angle measured on the equatorial plane eastward from the Vernal Equinox to the ascending node. The ascending node is the

point on the equator at which the satellite is leaving the Southern Hemisphere and entering the Northern Hemisphere. The right ascension varies from 0 to 360 degrees.  $\omega$  is the argument of perigee. It is the angle measured from the center of the Earth and is in the orbital plane in the direction of satellite motion from an ascending node to perigee.  $\omega$  is used to describe the orientation of a semi-major axis of an orbit relative to the equatorial plane. The argument of perigee varies from 0 to 360°. The last element,  $\theta$  (true anomaly) is the angle measured from perigee to the satellite's position vector in the direction of satellite motion. The true anomaly describes the satellite current position relative to the location of the perigee. Its value varies from 0 to 360°.

#### ***b. Circular Orbit***

The circular orbit can also be described by using the six of the classical orbital elements as mentioned earlier. However, some elements are ambiguous. Specifically, the circular orbit has no perigee, hence it has no argument of perigee and true anomaly, since both use the perigee as a reference point. Figure 2.4 illustrates the circular orbit. Note that if a circular orbit is considered as the limit of elliptical orbits, then the perigee and apogee can be specified as limits.

It is common to specify satellite position in circular orbit with polar coordinates (Colwell, 1983). The radius of satellite orbit,  $R$ , and the orbital true anomaly,  $\theta$ , are given by equation (2-3) and (2-4), respectively.

$$R = R_E + H_S \quad (2-3)$$

$$\theta = \dot{\theta} t \quad (2-4)$$

where  $R_E$  = radius of the Earth (6378 km)

$H_S$  = altitude of satellite

$t$  = time that a satellite travels from an ascending node to  
satellite position vector.

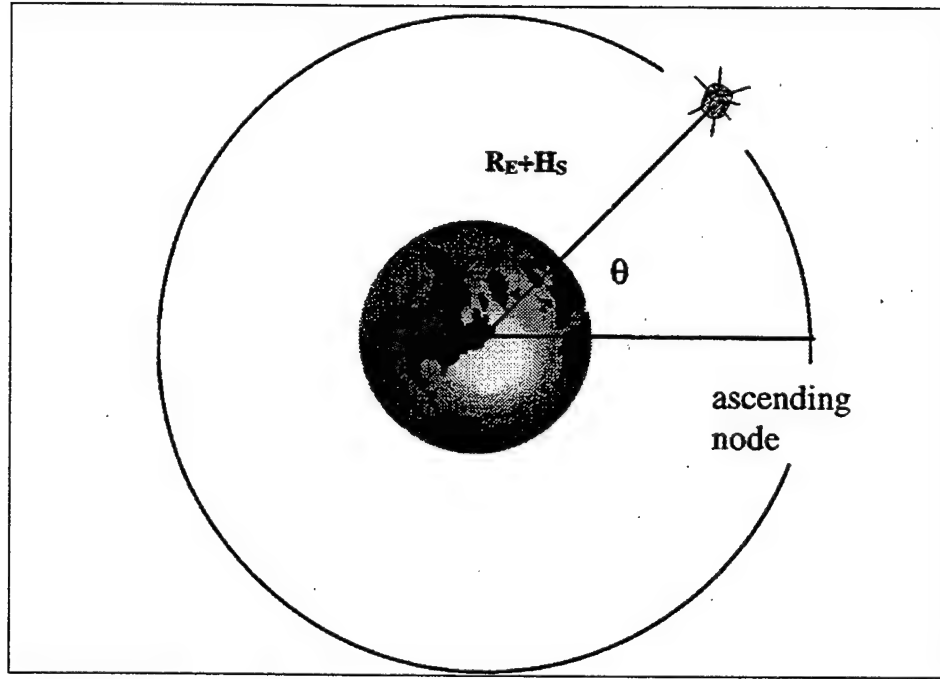


Figure 2.4 Circular Orbit

The angular velocity in circular orbit is given by

$$\dot{\theta} = \sqrt{\frac{\mu}{R^3}}, \quad (2-5)$$

and the corresponding orbital period,  $T$ , is

$$T = 2\pi \sqrt{\frac{R^3}{\mu}} \quad (2-6)$$

where  $\mu$  = Earth gravitational constant ( $3.9860 \times 10^{14} \text{ m}^3/\text{sec}^2$ )

#### 4. Satellite Ground Track

The satellite ground track is defined as the path of the subsatellite point over the Earth's surface (Colwell, 1983). Consider a satellite in a circular orbit at an altitude of  $H_s$  and inclination  $i$ . Figure 2.5 illustrates the spherical triangle for determining a subsatellite point. The latitude ( $\psi_s$ ) and longitude ( $L_s$ ) of a subsatellite point are determined from  $\theta$  by solving the spherical triangle NSL in Figure 2.5 to obtain,

$$\sin \psi_s = \sin i \sin \theta \quad (2-7)$$

$$\tan L_s = \cos i \tan \theta \quad (2-8)$$

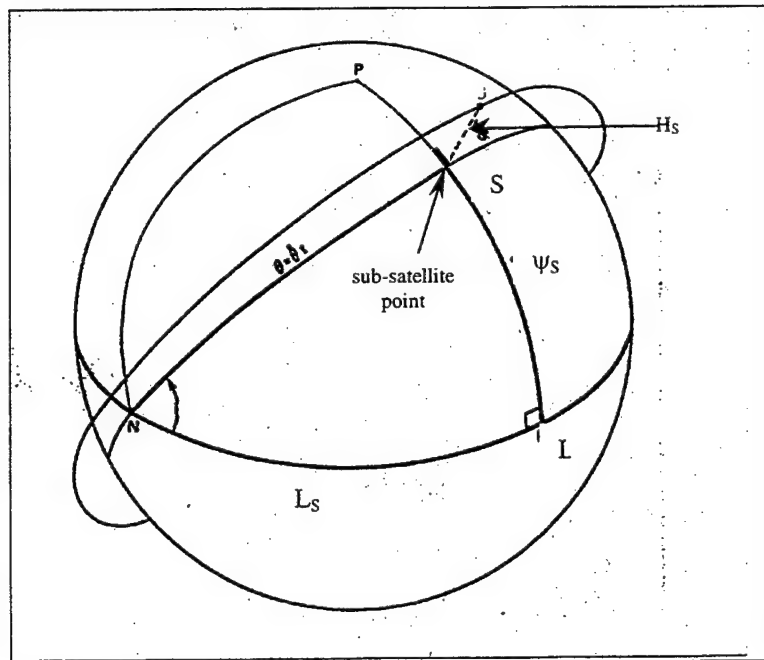


Figure 2.5 Determination of Subsattellite Point (Cowell, 1983)

## B. ORBITAL COVERAGE

The coverage region at any point in time is that part of the Earth which the satellite can “see”. For the simple case of a spherical cap coverage region, the boundary of the coverage region can be specified by the Earth central angle,  $\lambda$ , measured at the center of the Earth from subsatellite point to the target. Figure 2.6 illustrates this geometry. It is often the case that the maximum  $\lambda$  is determined by the minimum elevation angle,  $\xi$ , that allows the satellite to detect the target.

### 1. Target Elevation Constraint

A target is visible to a satellite only if the elevation angle  $\xi$ , measured at the target between the satellite and the local horizontal satisfies equations (2-9) or (2-10) (see Figure 2.6). For a satellite at altitude  $H_s$  and elevation angle  $\xi$ , the equation for  $\lambda$  is (Wilkinson, 1994):

$$\lambda = \frac{\pi}{2} - \xi - \sin^{-1} \left[ \frac{R_E \cos \xi}{R_E + H_s} \right], \quad (2-9)$$

$$= \cos^{-1} \left[ \frac{R_E \cos \xi}{R_E + H_s} \right] - \xi \quad (2-10)$$

### 2. Horizon Constraint

The maximum angular radius of the coverage region is  $\lambda_H$ , which satisfies

$$\cos \lambda_H = \frac{R_E}{R_E + H_s}. \quad (2-11)$$

Figure 2.6 illustrates the geometry of orbital coverage.

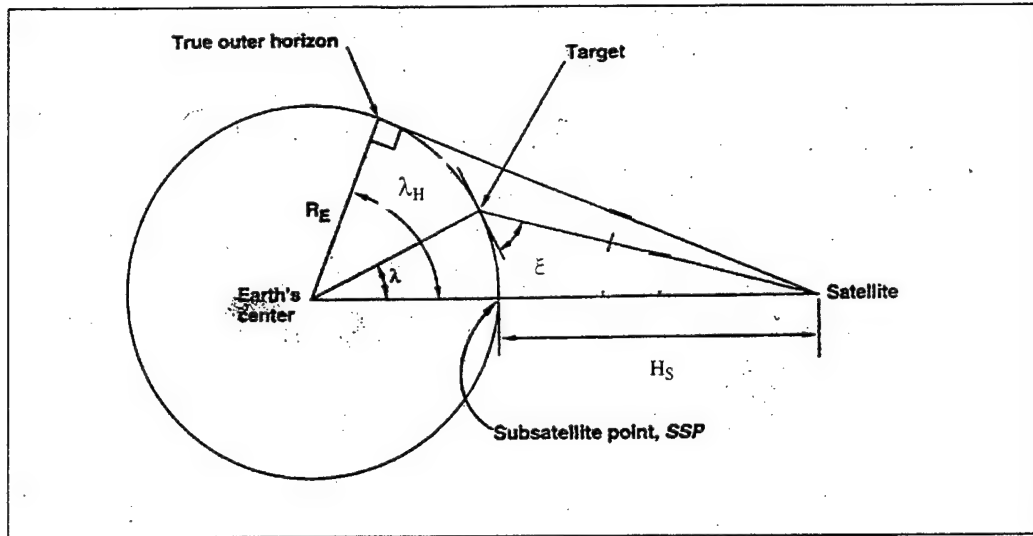


Figure 2.6 Coverage Angular Radius (Larson & Wertz, 1992)

## C. FRACTION OF COVERAGE EQUATIONS

### 1. Wertz's Equations

Wertz derives coverage as a function of latitude,  $\psi_T$ , for a satellite in a circular orbit at inclination  $i$  when Earth's rotation is ignored. He assumed that observations can be made at any angular distance less than or equal to  $\lambda_{max}$  on either side of the satellite ground track. The latitude is also assumed positive (i.e., in the northern hemisphere). "Depending on the latitude, there will be either no coverage, a single long region of coverage, or two shorter regions of coverage for each orbit as follows" (Larson & Wertz, 1992):

Latitude Range	Number of Coverage Regions	Percent Coverage	
$\lambda_{\max} + i < \psi_T$	0	0	(2-12a)
$i - \lambda_{\max} < \psi_T < i + \lambda_{\max}$	1	$\phi_1/180$	(2-12b)
$0 < \psi_T < i - \lambda_{\max}$	2	$\phi_2/180$	(2-12c)

where  $\cos \phi_1 = \frac{\cos i \sin \psi_T - \sin \lambda_{\max}}{\sin i \cos \psi_T}$ , and (2-13a)

$$\cos \phi_2 = \frac{\cos i \sin \psi_T + \sin \lambda_{\max}}{\sin i \cos \psi_T} \quad (2-13b)$$

where  $\phi_1$  and  $\phi_2$  are one-half the longitude range over which coverage occurs. Figure 2.7 illustrates regions of coverage for each orbit.

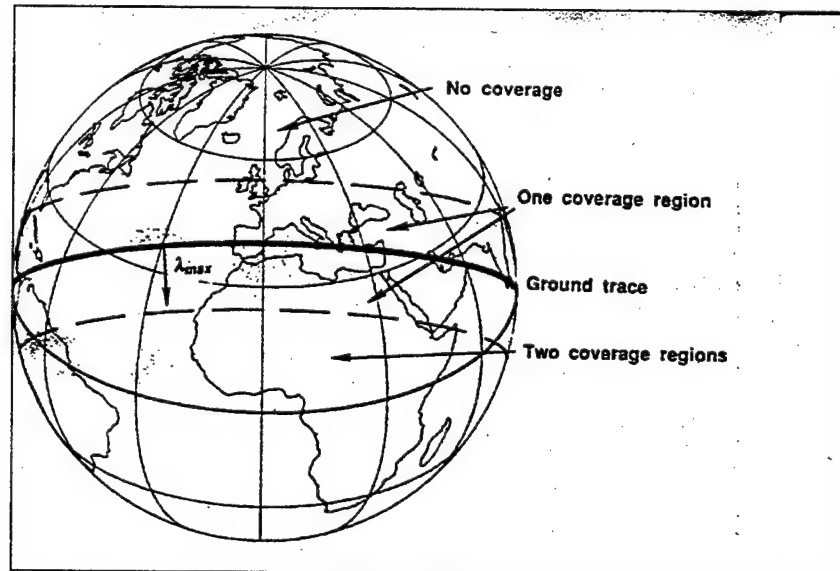


Figure 2.7 Regions of Coverage (Larson & Wertz, 1992)

## 2. Washburn's Equation

Washburn proposed a method to calculate the fraction  $g$  of latitude line covered during one satellite pass. If the target's longitude is uniformly distributed over the latitude line, this fraction is a probability of detection. Unlike Wertz's method, this derivation assumes a rotating Earth (Washburn, 1997).

Under the assumption that the radius of the satellite coverage is small (i.e.,  $\lambda_{\max} \ll \pi$ ), the fraction of latitude line covered as a function of  $\psi_T$ ,  $\omega_E$ ,  $i$ , and  $\lambda_{\max}$  is given by

$$g(\psi_T, \omega_E, i, \lambda_{\max}) = \frac{\lambda_{\max}}{\pi \sin \beta \cos \psi_T} \quad (2-14)$$

where  $\beta = \arctan\left(\frac{\sqrt{\sin^2 i - \sin^2 \psi_T}}{\cos i - \omega_E \cos^2 \psi_T}\right)$ ,  $\psi_T$  is target's latitude, and  $\psi_T < i$ . The angle  $\beta$  is

determined by the velocity of the satellite relative to the Earth. Earth's rotation rate,  $\omega_E$ ,

in terms of radians of rotation per radian of anomaly is determined by  $\omega_E = \frac{1}{Q}$ , where  $Q$

is the repetition factor.





### **III. MODEL DEVELOPMENT**

#### **A. GENERAL ASSUMPTIONS FOR MATHEMATICAL MODEL DEVELOPMENT**

A real satellite orbit can be quite complex. It is not exactly elliptical for many reasons, but mainly because of the Earth's equatorial bulge and atmospheric drag. However, in order to make our computation possible, some assumptions, but as few as possible, are made. In our work, the following assumptions are used:

- i.) the Earth is a sphere,
- ii.) the mass of a satellite is negligible compared to the mass of the Earth,
- iii.) the Earth and the satellite are the only two heavenly bodies in the system,
- and iv.) gravity is the only force acting along a line joining the centers of the Earth and the satellite.

The intent of this thesis is to develop an initial tool for evaluating a surveillance satellite so that the decision-maker can choose good orbital parameters for a particular mission. The primary emphasis is on circular orbit, as it is used in most military applications such as the space shuttle, geo-synchronous satellites, and sun-synchronous reconnaissance satellites (Friedman et al., 1985).

## B. DETECTION PARAMETERS

In a search and detection model of a surveillance satellite, the detection rate of the satellite ( $\rho$ ), defined as the mean number of detections per unit time, is a function of many variables. In this analysis, we assume that at time  $t$ ,

$$\rho(t) = f(\lambda(t), \beta_1(t), \beta_2(t)), \quad (3-1)$$

where

$\lambda(t)$  = angular distance between subsatellite point and target,

$\beta_1(t)$  = target azimuth angle, great circle bearing of the subsatellite point from the target, and

$\beta_2(t)$  = sensor azimuth angle, spherical angle measured at the subsatellite point between the direction of motion of the subsatellite point and the target. Figure 3.1 illustrates the above three variables.

Assuming that the times of detection are given by a Poisson process with rate  $\rho(t)$  at time  $t$ , the probability of a detection,  $P_d$ , in time interval  $[t_1, t_2]$  is

$$P_d(t_1, t_2) = 1 - e^{-\int_{t_1}^{t_2} \rho(t) dt} \quad (3-2)$$

In the following section, we will derive expressions for  $\lambda(t)$ ,  $\beta_1(t)$ , and  $\beta_2(t)$ .

### 1. Angular Distance

Washburn developed the following expression for the angular distance,  $\lambda$ , as a function of time (Washburn, 1997).

$$\lambda(t) = \cos^{-1}[\cos(\psi_T)\cos(L_T)\cos(\theta) + \cos(\psi_T)\sin(L_T)\cos(i)\sin(\theta) + \sin(\psi_T)\sin(i)\sin(\theta)] \quad (3-3)$$

where

$\psi_T$  = latitude of a target on the Earth,

$L_T$  = longitude of a target on the Earth, and

$\theta$  = orbital true anomaly.

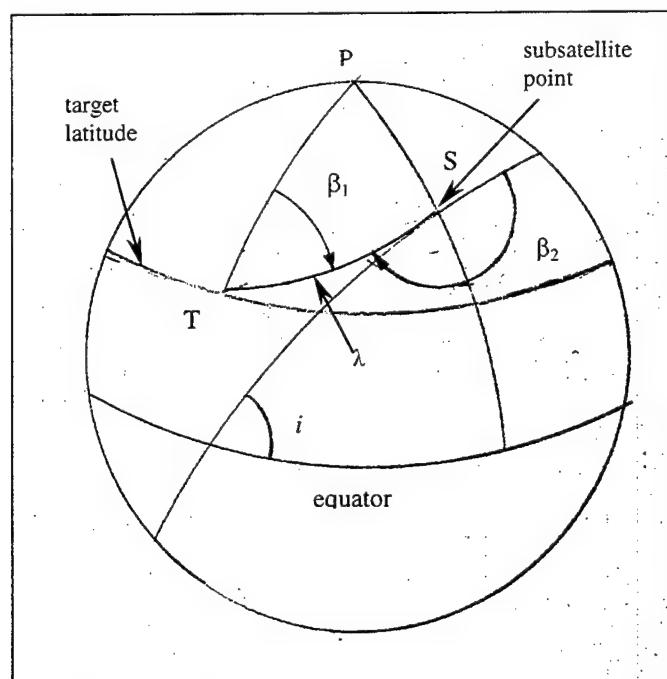


Figure 3.1 Detection Parameters

From equation (3-3), by taking the Earth's rotation into account, and assuming the target to be stationary, the geographical coordinate  $(\psi_T, L_T)$  of the target becomes

$$\begin{aligned} \psi_T &= \psi_0 \\ L_T &= L_0 + \frac{\theta}{Q} \end{aligned} \tag{3-4}$$

where  $Q$  is the number of satellite orbits that correspond to one rotation of the Earth (the repetition factor).  $\psi_0$  and  $L_0$  are the target's latitude and longitude when  $\theta = 0$ . Notice that the Earth's rotation only affects the longitude of the target.

As an example, consider a satellite with an orbital radius of 6700 kilometers, an inclination of  $50^\circ$ , and period of 5458 seconds. The target's latitude is  $10^\circ$  N and longitude at time  $t = 0$  is  $70^\circ$  W. The following figure shows the variation of the angular distance as a function of orbital true anomaly ( $\theta$ ).

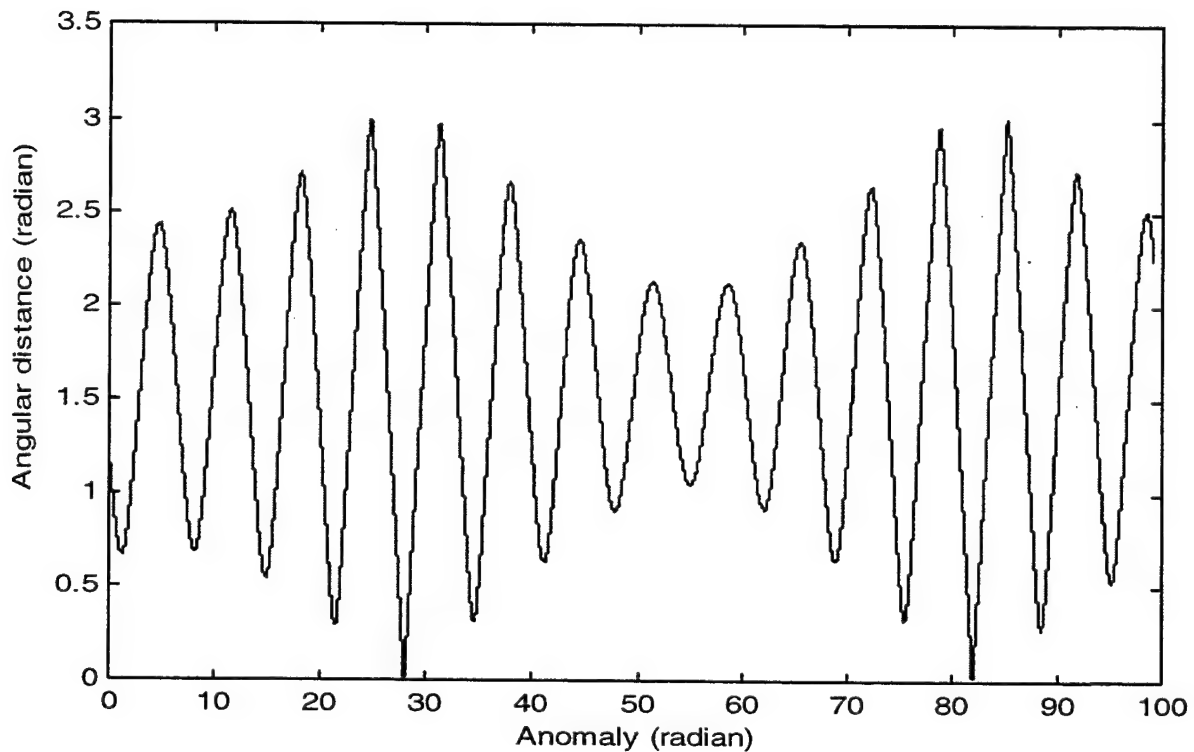


Figure 3.2. Angular Distance and Anomaly

The angular distance is a periodic function. If  $\psi_T < i$  and assuming a fixed orbital plane, then twice each sidereal day the target rotates through the satellite orbital plane, and "close" passes are possible.

## 2. Target Azimuth Angle

We now derive an analytical expression for target azimuth angle ( $\beta_I$ ). Our concept is that the target is visible to a satellite only if the target azimuth angle is appropriate. This models the fact that natural or man-made objects in the vicinity of the target can affect the detection rate.

Our convention is that the target azimuth angle  $\beta_l$  is measured eastward from north (in the Northern Hemisphere) from the target to the subsatellite point. Figure 3.3 illustrates the spherical triangle for determining the target azimuth angle  $\beta_l$ .

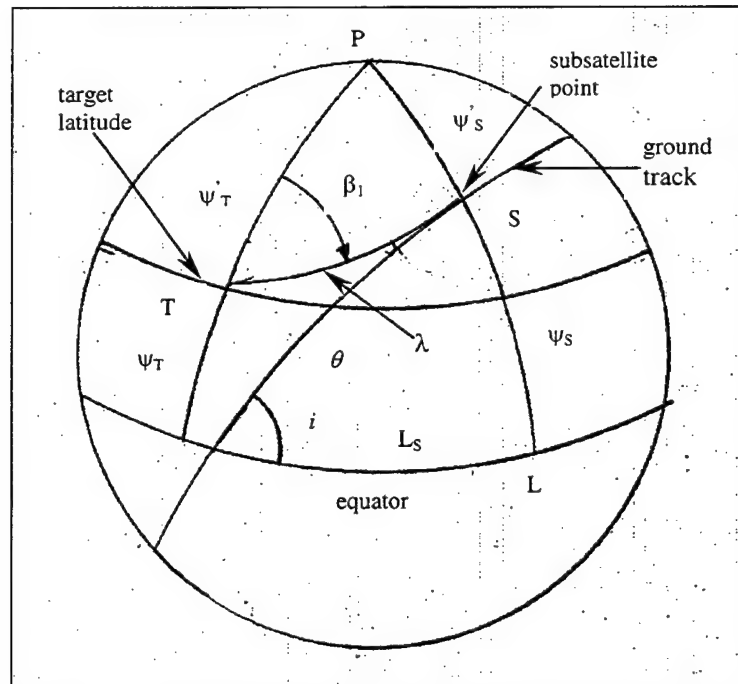


### Figure 3.3 Determination of Target Azimuth Angle

Given geographic coordinates of a target,  $\psi_T$  and  $L_T$ , and a position of the subsatellite point ( $\psi_S, L_S$ ). The target azimuth angle can be expressed mathematically as the following equation (see also APPENDIX B).

$$\beta_1 = \cos^{-1} \left[ \frac{\sin(\theta) \sin(i) - \sin(\psi_T) \cos(\lambda)}{\cos(\psi_T) \sin(\lambda)} \right], \quad (3-5)$$

where  $\theta$  is calculated by equation (2-4) and the angular distance ( $\lambda$ ) is determined by equation (3-3).  $\beta_1$  is less than 180 degrees if target is west of the subsatellite point, and greater than 180 degrees if target is east of the subsatellite point.

### 3. Sensor Azimuth Angle

A detection can occur only if the satellite's sensors are pointed towards the target. More generally, we assume that the detection rate,  $\rho$ , is a function of the sensor azimuth angle,  $\beta_2$ . This allows modeling of the satellite sensors which are not omni-directional, such as in a side-looking airborne radar (SLAR) (Larson and Wertz, 1992).

An expression for  $\beta_2$  can be derived by solving the spherical triangle PTS and PAS, using the spherical trigonometry Law of Cosine for Sides (see Figure 3.4).

Assuming that geographical coordinates of a subsatellite point and a target are known,  $\beta_2$  can be expressed as (see also APPENDIX C)

$$\beta_2 = 2\pi - (\eta + \alpha), \quad (3-6)$$

where  $\eta$  and  $\alpha$  are

$$\eta = \cos^{-1} \left[ \frac{\sin(\psi_T) - \sin(\psi_S) \cos(\lambda)}{\cos(\psi_S) \sin(\lambda)} \right], \quad (3-7)$$

$$\alpha = \sin^{-1} \left[ \frac{\cos(i)}{\cos(\psi_S)} \right]. \quad (3-8)$$

Here  $\psi_S$  (latitude of subsatellite point) is determined by equation (2-7).





say that the probability of detection during a particular satellite pass is only a function of the minimum angular separation (or “lateral range”) between the target and the subsatellite point.

In this work, we present a procedure for determining the minimum angular distance occurring during one satellite pass. Then we can use a sensor’s lateral range curve to find a probability of detection. The lateral range curve,  $l(x)$ , is the conditional probability of detection, given that target’s range at CPA is  $x$  (in this case,  $\lambda_{min}$ ). The lateral range curve is neither a probability density function nor a cumulative distribution function. It is a plot of conditional probabilities which depend on the target, environmental conditions and the satellite sensors. (United States Naval Institute, Naval Operation Analysis, 1989)

#### **D. MINIMUM VALUE OF ANGULAR DISTANCE**

To approximate probability of detection by applying the satellite’s sensor lateral range curve, the most important step is to determine the range of a target at CPA. We have been unable to find an analytical expression for the minimum value of angular distance ( $\lambda_{min}$ ). But we can use numerical methods to approximate the solution. After trying several procedures, Newton’s method was selected, since the function of  $\lambda(t)$  is nonlinear, but the second derivative is available.

Newton’s method is based on exploiting the quadratic approximation of the function  $\lambda$  at a given point  $\theta_k$  (Bazaraa, Sherali, & Shetty, 1993). This quadratic approximation  $q$  is given by

$$q(\theta) \approx \lambda(\theta_k) + \lambda'(\theta_k)(\theta - \theta_k) + \frac{1}{2} \lambda''(\theta_k)(\theta - \theta_k)^2 \quad (3-11)$$

The point  $\theta_{k+1}$  is taken to be the point where the derivative of  $q$  is equal to zero. This yields

$$\lambda'(\theta_k) + \lambda''(\theta_k)(\theta_{k+1} - \theta_k) = 0 \quad (3-12)$$

so that,

$$\theta_{k+1} = \theta_k - \frac{\lambda'(\theta_k)}{\lambda''(\theta_k)}. \quad (3-13)$$

The following is a summary of Newton's method to find the angular distance function  $\lambda$ .

*Initialization Step:* Choose a scalar  $\varepsilon \ll 1$  to be used for terminating the iterations.

Choose the initial point at anomaly  $\theta_I$ , sufficiently close to optimal value  $\hat{\theta}$ , found by graphing the angular distance against the orbital true anomaly  $\theta$  (see Figure 3.2). The CPA is in general different for every pass of a satellite over a target, so it is necessary to provide an initial value for the method for every satellite pass. The second initial value is the first optimal value  $\hat{\theta}_1$  plus  $2\pi$ . The third initial value is the second optimal value  $\hat{\theta}_2$  plus an interval between the first and second optimal values,  $(\hat{\theta}_2 - \hat{\theta}_1)$ , and so on.

*Main Step:*

1. Let  $\theta_k = \theta_I$  and evaluate  $\lambda'(\theta_k)$  and  $\lambda''(\theta_k)$ .
2. Let  $\theta_{k+1} = \theta_k - \frac{\lambda'(\theta_k)}{\lambda''(\theta_k)}$ .

The procedure is terminated when  $\|\theta_{k+1} - \theta_k\| < \varepsilon$ . Otherwise, replace  $k$  by  $k+1$  and repeat step 1.

*Checking Step:* Let  $\hat{\theta} = \theta_{k+1}$  and evaluate  $\lambda''(\hat{\theta})$ . If  $\lambda''(\hat{\theta}) > 0$ , the optimal value occurs at  $\hat{\theta}$ , and then the minimum  $\lambda$  is determined by evaluating  $\lambda$  at  $\hat{\theta}$ .

As an example, suppose a satellite is in circular orbit at an altitude of 6640.4 km, an inclination of  $65^\circ$ , period of 5385.3 seconds, and  $Q$  of 16. A target will be assumed at geographical coordinates of ( $\psi_T = 55^\circ$ ,  $L_T = 120^\circ$ ). Figure 3.5 shows the relationship between the angular distance and the anomaly.

Now, evaluate the minimum value of the angular distance  $\lambda_{min}$  by using Newton's algorithm. From equation (2-11) with horizon constraint, a detection is possible if the range of a target is less than or equal to 0.311 radian ( $\lambda_{max}$ ) on either side of satellite ground track. The lateral range curve of the sensor mounted on the satellite is assumed to be

$$\begin{aligned} l(x) &= 0.25e^{-0.25|x|}, \text{ if } -0.311 \leq x \leq 0.311 \\ &= 0, \text{ otherwise} \end{aligned} \tag{3-14}$$

where  $x$  is the lateral range or the range at CPA.

The numerical values for this problem are shown in the table below. Figure 3.6 shows the probability of the target being detected versus CPA time. Figure 3.7 illustrates the cumulative probability of detection (CPD) in one sidereal day. In this example, the satellite makes 16 orbits in one sidereal day. Therefore, the ground track of the subsatellite point repeats each sidereal day, as do the target detection probabilities.

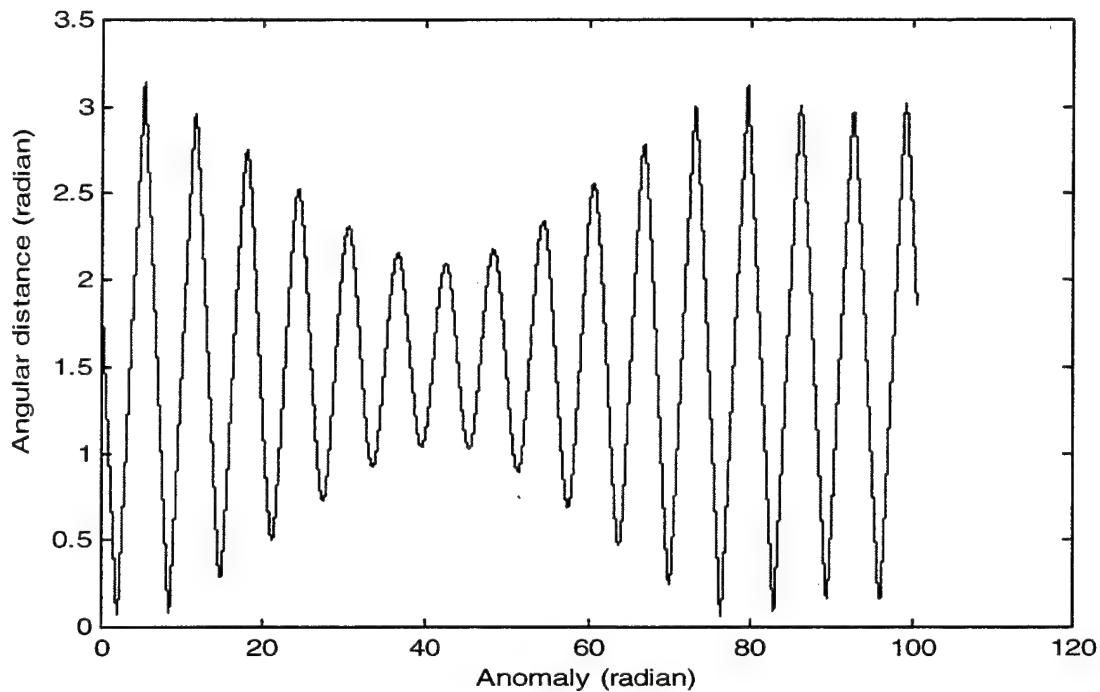


Figure 3.5 Angular Distance against Anomaly

pass	anomaly (radian)	time (min)	CPA (radian)	probability of detection	cumulative probability of detection
1	2.01	28.7	0.1077	0.2434	0.243
2	8.30	118.6	0.1124	0.2431	0.427
3	14.76	210.8	0.2857	0.2328	0.561
4	21.09	301.2	0.5069	0.0000	0.561
5	27.33	390.3	0.7282	0.0000	0.561
6	33.45	477.8	0.9201	0.0000	0.561
7	39.43	563.2	1.0351	0.0000	0.561
8	45.34	647.6	1.0238	0.0000	0.561
9	51.34	733.4	0.8919	0.0000	0.561
10	57.48	821.2	0.6924	0.0000	0.561
11	63.74	910.5	0.4694	0.0000	0.561
12	70.07	1000.9	0.2504	0.2348	0.664
13	76.40	1091.3	0.0939	0.2442	0.746
14	82.86	1183.6	0.1133	0.2430	0.808
15	89.41	1277.3	0.1682	0.2397	0.854
16	95.97	1370.9	0.1602	0.2402	0.889

Table 3.1 Closest Point of Approach and Probability of Detection

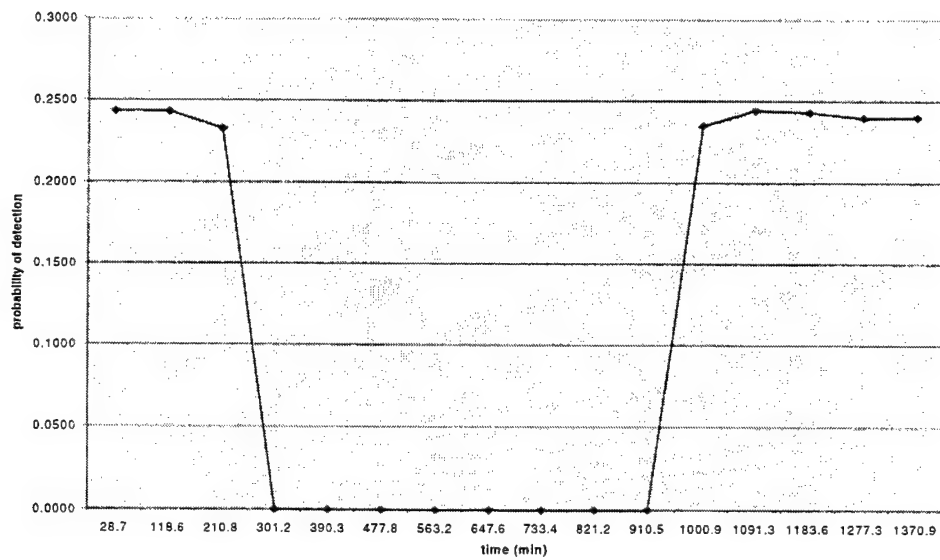


Figure 3.6 Probability of Detection versus Time

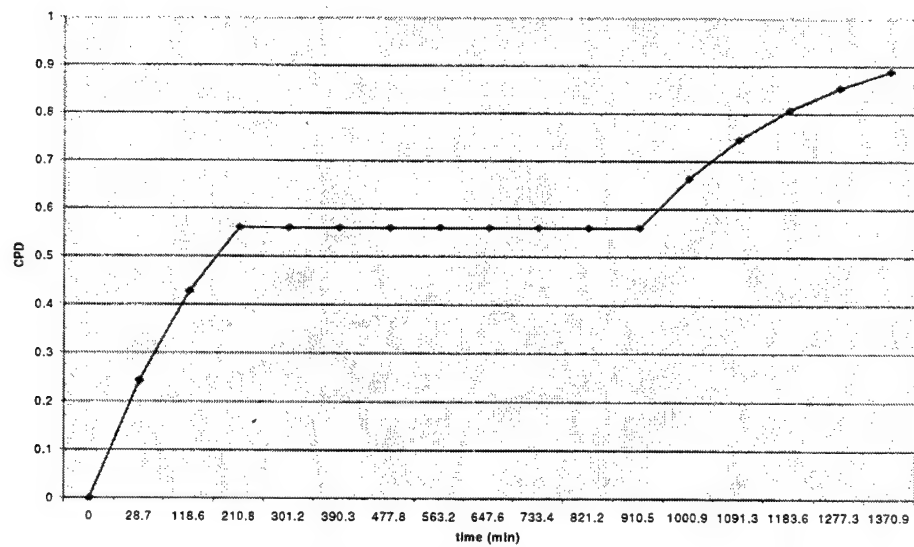


Figure 3.7 Cumulative Probability of Detection versus Time

## IV. EXPERIMENTATION AND RESULT

### A. EXPERIMENTATION

In this section, we test four analytical models for estimating the probability of detection of a target by a surveillance satellite. We will look at two lateral range curve models, an Earth coverage model developed by Wertz, and the detection rate model proposed by Washburn.

For the lateral range curve models, the probability of detection,  $p_{ave}$ , is

$$p_{ave} = \frac{\sum_{i=1}^k p_i}{k} \quad (4-1)$$

where  $p_i$  is the probability of detection at the  $i^{\text{th}}$  CPA, and  $k$  is the number of CPA's occurring during one "repetition period" of satellites orbits. That is, if the repetition factor  $Q$  is rational and equal to  $\frac{m}{n}$ , where  $m$  and  $n$  are positive integers, then exactly  $m$  orbits occur in  $n$  sidereal days. And then  $k$  is the number of CPA's occurring in either  $m$  orbits or  $n$  days.

From the fact that detection is possible only if the angular distance is within a specified field-of-view (FOV) of the satellite, the satellite can detect the target only if the range to the target is less than or equal to  $\lambda_{max}$  on either side of satellite ground track. To compare the solutions resulting from these four models, we have assumed that  $\lambda_{max}$  is equal in all computations. We have chosen to investigate a satellite at altitude  $H_S$  of 262.4 km (radius of satellite orbit = 6,640.4 km) with the inclination  $i$  of  $65^\circ$ , period  $T$  of

5385.3 seconds, and  $Q$  of 16. This is because most surveillance satellites are in low earth orbit at an altitude of less than 2000 km, and an inclination between  $60^\circ$  to  $104^\circ$  (Vallado, 1997). A satellite orbiting in this inclination ranges will cover the largest portion of the Earth. For communications, the elevation angle from the target horizon must be more than  $5^\circ$  (Larson and Wertz, 1992). In our problem, the satellite's assumed minimum useable elevation angle is  $10^\circ$ , resulting in a maximum angular distance ( $\lambda_{max}$ ) of 0.174 radian from equation (2-10).

For the first two models, Newton's method (explained in Chapter III) is used to compute  $k$  minimum angular distance values for each chosen latitude. The target's latitude and longitude and the sensor's lateral range curve are assumed to be known.

In the first model, we assume the sensor's lateral range curve is

$$l_1(x) = \begin{cases} 0.85e^{-0.85|x|} & , \text{ if } -0.174 \leq x \leq 0.174 \\ 0 & , \text{ otherwise} \end{cases} \quad (4-2)$$

where  $x$  is the angular distance in radians at the closest point of approach (CPA). This function will provide a probability of detection for each angular distance at the CPA. Figure 4.1 illustrates the lateral range curve  $l_1(x)$ .

In the second model, we assume that the sensor's lateral range curve is that of a cookie-cutter sensor. The probability is equal to 1 when the target is within the  $-\lambda_{max}$  to  $\lambda_{max}$ . So,

$$l_2(x) = \begin{cases} 1 & \text{if } -0.174 \leq x \leq 0.174 \\ 0 & \text{otherwise} \end{cases} \quad (4-3)$$

where  $x$  is the angular distance at CPA.

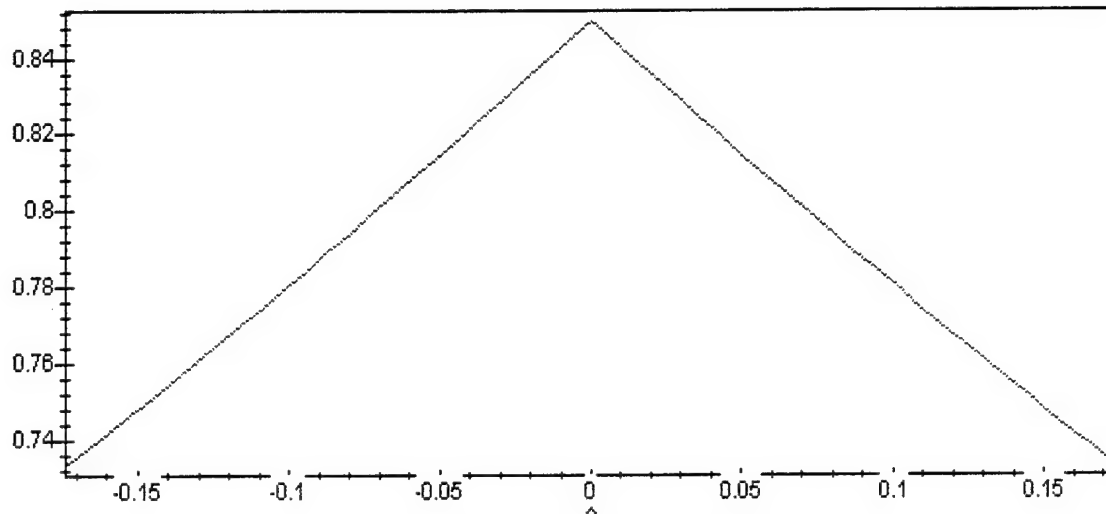


Figure 4.1 Lateral Range Curve

In the third model, we again assume that  $\lambda_{max}$  is equal to 0.174 radian. Also, we assume that the target is uniformly distributed over longitude, in order to make the percent coverage a probability of detection. Equations (2-12a) to (2-13b) are used to compute the percent coverage as a function of latitude for both the one-coverage region and two-coverage region (mentioned earlier in Chapter II). For this particular problem, the one-coverage region covers from latitudes  $55^\circ$  to  $75^\circ$  ( $i - \lambda_{max}$  to  $i + \lambda_{max}$ ), and the two-coverage region covers from  $0^\circ$  to  $55^\circ$  ( $i - \lambda_{max}$ ). The no-coverage region falls into the latitude range greater than  $75^\circ$  ( $i + \lambda_{max}$ ).

In the last model (equation (2-14)), the same  $\lambda_{max}$  (0.174 radian) is used to compute the fraction of the latitude line passing through the target that is covered by the satellite sensor. Following Washburn's concept, the target's longitude is assumed to be



uniformly distributed, and the fraction of the latitude line covered becomes a probability of detection.

Although the probability of detection can be computed continuously along the orbit at all latitudes, target latitudes of 0, 15, 30, and 50 degrees in the two-coverage region; 55, 64, 65, and 70 degrees in the one-coverage region; and 75, and 80 degrees in the no-coverage region are chosen for the demonstration of Model 3. These target latitudes are also used for the computations of Models 1, 2, and 4, so that the results are comparable. Notice that targets in this work are located only in the Northern Hemisphere. The same technique can be used to compute the probability of detection in the Southern Hemisphere.

## B. RESULTS

The results of the computations are tabulated in Table 4.1. The probability of detection for Model 1 (second column in Table 4.1) increases as the target's latitude increases from 0°, and it reaches the maximum probability at the latitude of 55°. After 55°, the probability decreases and becomes zero when the target's latitude is greater than or equal to 75°, which coincides with  $i + \lambda_{max}$ . If we borrow the one-, two-, and no-coverage region definitions from Model 3 to discuss Model 1's results, we can say the following. The Model 1 probability of detection increases until it reaches a maximum value at the northern edge of the two-coverage region ( $0 < \psi_T < i - \lambda_{max}$ ). The Model 1 probability then decreases, reaching 0 at the northern edge of the one-coverage region.

Target's latitude	Model 1 $l_1(x) = 0.85e^{-0.85x}$	Model 2 $l_2(x) = \begin{cases} 1, & \text{if } 0.174 \leq x \leq 0.174 \\ 0 & \text{otherwise} \end{cases}$	Model 3	Model 4
0	0.103	0.133	0.122	0.119
15	0.108	0.133	0.128	0.124
30	0.142	0.188	0.147	0.143
50	0.191	0.250	0.242	0.223
55	0.286	0.375	0.378	0.278
64	0.251	0.313	0.326	0.926
65	0.249	0.313	0.315	NA
70	0.190	0.250	0.243	NA
75	0.000	0.000	0	NA
80	0.000	0.000	0	NA

Table 4.1 Average Probability of Detection

The Model 2 probabilities of detection (column 3 in Table 4.1) are 0.133 for target latitude  $0^\circ$  and  $15^\circ$ , and then increase to a maximum value of 0.375 for a target latitude of  $55^\circ$  (first point of the one-coverage region). The Model 2 probabilities of detection then decrease with increasing target latitude until  $75^\circ$  (the most southern latitude in the no-coverage region), where it becomes 0.

We note that for the first and second models, there can be more CPA's than orbits. This happens because two CPA's are possible during the orbit where the angular separation between the target and the orbital plane is maximal. However, the probability of detection is zero in this orbit because the angular distance is generally greater than  $\lambda_{max}$ .

In the third model (Wertz's model), the probability of detection behaves in the same way as in the first model. That is, it increases with target latitude. It reaches the maximum value at  $55^\circ$ , the most southern latitude of the one-coverage region. Then, it decreases for target latitudes greater than  $55^\circ$ , until it becomes zero at  $75^\circ$ . The same

explanation regarding the one-, two-, and no-coverage regions discussed in the second model is also valid here.

The probability of detection in Model 4 (Washburn's model) increases and decreases in a different way from the others. As shown in column 4 of Table 4.1, it keeps increasing monotonically with the target latitude until becoming indeterminate for latitude equal to the orbital inclination of  $65^\circ$ . This occurs because angle  $\beta$  in equation (2-14) becomes 0 at  $\psi_T = 65^\circ$ , which causes the denominator to vanish.

### C. DISCUSSION OF RESULTS

The probabilities of detection at the same target latitude are different when using the four different models. Model 3 by Wertz is commonly used and is well-known. It assumes a non-rotating Earth. This is reasonable for a satellite in a very low orbit where the Earth's rotation can be ignored. The probability of detection computed from this model always has the same value for the same target latitude regardless of environmental conditions, the target's longitude, and the satellite ground track position. One should probably expect a change in the probability of detection for different ground track positions, but this does not occur for Models 3 and 4.

In our newly developed techniques (Models 1 and 2), the probability of detection follows the same pattern as that of Model 3. The Models 1 and 2 results are close but not exactly equal to those of Model 3, because we have used a specific lateral range curve. In a real military mission, a different lateral range curve would be used.

An important feature of Models 1 and 2 is that the probabilities of detection change as the satellite ground track is changed. Depending on the application, this could be an improvement over Models 3 and 4. The variation of the probability of detection with respect to the satellite ground track location is useful when one needs to know the detection probability for a specific target location instead of an average one over an entire latitude line.

In Models 1, 2, and 3, the probability of detection in the one-coverage region is relatively higher than that of the two-coverage region. The high probability in the one-coverage region agrees well with Clark's (1966) and Washburn's (1997) observations. They have shown by the mathematical formulations that the time that a satellite spends at the extreme latitudes is greater than at the lower latitudes. They have also suggested that a target whose latitude is slightly smaller than  $i$  (i.e., in the one-coverage region) should be easiest to find. This is because the density of the satellite's latitude (defined by Washburn (1997)) is greatest there.

In Model 4 by Washburn, the Earth's rotation has been taken into account. The probability of detection is computed in a conceptual manner similar to the Wertz technique. While the Wertz technique takes the percentage of coverage as the probability of detection, Washburn takes the fraction of the latitude line covered as this probability. This results in the probability of detection always having the same value for targets at the same latitude, regardless of environmental conditions, and the target longitude. Also, when the target latitude ( $\psi_T$ ) is equal to the satellite inclination ( $i$ ), equation (2-14) gives an indeterminate value. It is preferable that Washburn's technique be applied when

$\lambda_{max} < \pi$  (Washburn, 1997). It is also observed that the Model 4 probability of detection is close to 1 when  $\psi_T$  approaches  $i$ . This apparently suggests that the satellite almost completely covers the latitude line. A potentially more accurate model would have been

$$g = \min\left(\frac{W}{2\pi R \cos \psi_T}, \frac{L}{2\pi R \cos \psi_T}\right) \quad (4-4)$$

where  $L$  is the length of the satellite sensor foot print.

## V. CONCLUSIONS

### A. CONCLUSIONS

Satellite surveillance systems play a significant role in today's search and detection missions. Probability of detection is a useful measure of effectiveness for satellite surveillance systems. Wertz (1992) and Washburn (1997) proposed two analytical models to estimate the probability of detection. This thesis work developed a new mathematical formulation to improve on the Wertz and Washburn models.

The new methods proposed here are based on the classical search ideas of detection rate and lateral range curves. The new methods are preferred over the Wertz and Washburn methods when it is desired that the satellite model be sensitive to the target's longitude, environmental and geographic conditions in the vicinity of the target, or azimuthal sensitivity of the satellite sensor.

### B. SUGGESTION FOR FURTHER STUDIES

Possible areas of future work include:

- Investigating functional forms for  $\rho(t) = f(\lambda(t), \beta_1(t), \beta_2(t))$ , which are realistic and specific to a particular sensor/target system.
- Finding an analytical expression for the minimum value of angular CPA distance.



## APPENDIX A: SPHERICAL GEOMETRY FORMULAS

This appendix provides a summary of basic rules. [Extracted from Larson & Wertz, Space Mission Analysis and Design, 1992].

A right spherical triangle is one with at least one right angle. Any two of the remaining components, including the two remaining angles, serve to completely define the triangle. Napier's Rules provides a concise formulation for all possible right spherical triangles. These are listed below.

An oblique spherical triangle has arbitrary sides and angles. Sides and angles are generally defined over the range of 0 to 180 degrees, although most of the spherical geometry relations continue to hold in the angular range up to 360 degrees. A set of basic rules which can be applied to any spherical triangle are given below. Finally, these general rules can be used to write explicit expressions for any of the unknown components in any oblique spherical triangle with any three components known.

### RIGHT SPHERICAL TRIANGLES

In Table A1, the line below each formula indicates the quadrant of the answer.  $Q(A)=Q(a)$  means that the quadrant of angle  $A$  is the same as that of side  $a$ . "Two possible solution" means that either quadrant provides a correct solution to the triangle defined.



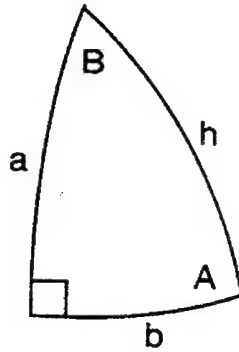


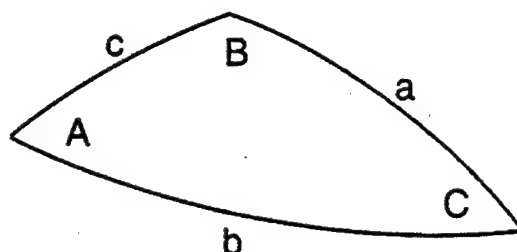
Table A1 Right Spherical Triangles [Larson & Wertz, 1992]

Given	Find		
a, b	$\cos h = \cos a \cos b$ $Q(h) = \{Q(a) Q(b)\}^*$	$\tan A = \tan a / \sin b$ $Q(A) = Q(a)$	$\tan B = \tan b / \sin a$ $Q(B) = Q(b)$
a, h	$\cos b = \cos h / \cos a$ $Q(b) = \{Q(a)/Q(h)\}^{**}$	$\sin A = \sin a / \sin h$ $Q(A) = Q(a)$	$\cos B = \tan a / \tan h$ $Q(B) = \{Q(a)/Q(h)\}^{**}$
b, h	$\cos a = \cos h / \cos b$ $Q(a) = \{Q(b)/Q(h)\}^{**}$	$\cos A = \tan b / \tan h$ $Q(A) = \{Q(b)/Q(h)\}^{**}$	$\sin B = \sin b / \sin h$ $Q(B) = Q(b)$
a, A	$\sin b = \tan a / \tan A$ Two possible solutions	$\sin h = \sin a / \sin A$ Two possible solutions	$\sin B = \cos A / \cos a$ Two possible solutions
a, B	$\tan b = \sin a \tan B$ $Q(b) = Q(A)$	$\tan h = \tan a / \cos B$ $Q(h) = \{Q(a)Q(B)\}^*$	$\cos A = \cos a \sin B$ $Q(A) = Q(a)$
b, A	$\tan a = \sin b \tan A$ $Q(a) = Q(A)$	$\tan h = \tan b / \cos A$ $Q(h) = \{Q(b)Q(A)\}^*$	$\cos B = \cos b \sin A$ $Q(B) = Q(b)$
b, B	$\sin a = \tan b / \tan B$ Two possible solutions	$\sin h = \sin b / \sin B$ Two possible solutions	$\sin A = \cos B / \cos b$ Two possible solutions
h, A	$\sin a = \sin h \sin A$ $Q(a) = Q(A)$	$\tan b = \tan h \cos A$ $Q(b) = \{Q(A)/Q(h)\}^{**}$	$\tan B = 1 / \cos h \tan A$ $Q(B) = \{Q(A)/Q(h)\}^{**}$
h, B	$\sin b = \sin h \sin B$ $Q(b) = Q(B)$	$\tan a = \tan h \cos B$ $Q(a) = \{Q(B)/Q(h)\}^{**}$	$\tan A = 1 / \tan A \tan B$ $Q(A) = \{Q(B)/Q(h)\}^{**}$
A, B	$\cos a = \cos A / \sin B$ $Q(a) = Q(A)$	$\cos b = \cos B / \sin A$ $Q(b) = Q(B)$	$\cos h = 1 / \tan A \tan B$ $Q(h) = \{Q(A)Q(B)\}^*$

\*  $\{Q(x)Q(y)\} \equiv 1^{\text{st}}$  quadrant if  $Q(x) = Q(y)$ ,  $2^{\text{nd}}$  quadrant if  $Q(x) \neq Q(y)$

\*\*  $\{Q(x)/Q(h)\} \equiv$  quadrant of  $x$  if  $h \leq 90$  deg, opposite quadrant of  $x$  if  $h > 90$  deg.

## OBLIQUE SPHERICAL TRIANGLES



The following rules hold for any spherical triangle:

The Law of Sines:

$$\frac{\sin a}{\sin A} = \frac{\sin b}{\sin B} = \frac{\sin c}{\sin C}$$

The Law of Cosines for Sides:

$$\begin{aligned}\cos a &= \cos b \cos c + \sin b \sin c \cos A \\ \cos b &= \cos c \cos a + \sin c \sin a \cos B \\ \cos c &= \cos a \cos b + \sin a \sin b \cos C\end{aligned}$$

The Law of Cosines for Angles:

$$\begin{aligned}\cos A &= -\cos B \cos C + \sin B \sin C \cos a \\ \cos B &= -\cos C \cos A + \sin C \sin A \cos b \\ \cos C &= -\cos A \cos B + \sin A \sin B \cos c\end{aligned}$$



## APPENDIX B: FORMULATION OF TARGET AZIMUTH ANGLE

From Figure 3.3, a target azimuth angle is given by equation (3-5). To derive this equation, we assume the target's coordinates (latitude  $\psi_T$ , longitude  $L_T$ ), are known. Latitude  $\psi_S$ , and longitude  $L_S$  of a subsatellite point are governed by equations (2-7), and (2-8), respectively. An angular distance  $\lambda$  is determined by equation (3-3). The target azimuth angle is accomplished by solving the spherical triangle PTS using the law of cosines for the sides. The equation is

$$\cos\left(\frac{\pi}{2} - \psi_S\right) = \cos\left(\frac{\pi}{2} - \psi_T\right) \cos \lambda + \sin\left(\frac{\pi}{2} - \psi_T\right) \sin \lambda \cos \beta_1 \quad (\text{B-1})$$

$$\sin \psi_S = \sin \psi_T \cos \lambda + \cos \psi_T \sin \lambda \cos \beta_1 \quad (\text{B-2})$$

Rearranging equation (B-2),

$$\cos \beta_1 = \frac{\sin \psi_S - \sin \psi_T \cos \lambda}{\cos \psi_T \sin \lambda} \quad (\text{B-3})$$

Substituting equation (2-7) into equation (B-3), and solving for  $\beta_1$ , the target azimuth angle becomes

$$\beta_1 = \cos^{-1} \left[ \frac{\sin \theta \sin i - \sin \psi_T \cos \lambda}{\cos \psi_T \sin \lambda} \right] \quad (\text{B-4})$$



## APPENDIX C: FORMULATION OF SENSOR AZIMUTH ANGLE

From Figure 3.4, a sensor azimuth angle  $\beta_2$  can be determined by equation (3-6).

To derive this equation, we need to determine the angle  $\alpha$ , and angle  $\eta$ .

First, we derive the angle  $\alpha$ . This is accomplished by solving the spherical triangle, PSA, using the right spherical triangle.

$$\sin \alpha = \frac{\sin a}{\sin(\frac{\pi}{2} - \psi_s)} \quad (C-1)$$

Substituting  $a$  with  $\frac{\pi}{2} - i$ , equation (C-1) becomes

$$\sin \alpha = \frac{\sin(\frac{\pi}{2} - i)}{\sin(\frac{\pi}{2} - \psi_s)} = \frac{\cos i}{\cos \psi_s} \quad (C-2)$$

Hence,

$$\alpha = \sin^{-1}\left(\frac{\cos i}{\cos \psi_s}\right) \quad (C-3)$$

Finally, we derive a formular for the angle  $\eta$ . This is also accomplished by solving the spherical triangle, PTS, using the spherical law of cosine for a side. A subsatellite point latitude  $\psi_s$ , and an angular distance  $\lambda$  are governed by equations (2-7), and (3-3), respectively. The angle  $\eta$  can be expressed as follows.

$$\cos\left(\frac{\pi}{2} - \psi_T\right) = \cos\left(\frac{\pi}{2} - \psi_s\right) \cos \lambda + \sin\left(\frac{\pi}{2} - \psi_s\right) \sin \lambda \cos \eta \quad (C-4)$$

$$\sin \psi_T = \sin \psi_s \cos \lambda + \sin \psi_s \sin \lambda \cos \eta \quad (C-5)$$

$$\cos \eta = \frac{\sin \psi_T - \sin \psi_S \cos \lambda}{\cos \psi_S \sin \lambda} \quad (\text{C-6})$$

$$\eta = \cos^{-1} \left( \frac{\sin \psi_T - \sin \psi_S \cos \lambda}{\cos \psi_S \sin \lambda} \right) \quad (\text{C-7})$$

Therefore, the expression of  $\beta_2$  is

$$\beta_2 = 2\pi - \eta + \alpha \quad (\text{C-8})$$

## APPENDIX D: FIRST AND SECOND DERIVATIVES

The first and second derivatives of equation (3-3) are:

$$\frac{d\lambda}{d\theta} = \lambda'(\theta) = \frac{\left( \frac{A \cos(\theta)}{Q} + B \sin(\theta) - \frac{B \cos(\theta)}{Q} - A \cos(i) \cos(\theta) - \sin(\psi) \sin(i) \cos(\theta) \right)}{\sqrt{1 - (B + A \cos(i) \sin(\theta) + \sin(\psi) \sin(i) \sin(\theta))^2}} \quad (D-1)$$

$$\frac{d^2\lambda}{d\theta^2} = \lambda''(\theta) = \frac{\left( \frac{B \cos(\theta)}{Q^2} - 2 \frac{A \sin(\theta)}{Q} + D + \frac{A \cos(i) \sin(\theta)}{Q^2} - 2 \frac{B \cos(i) \cos(\theta)}{Q} + C \sin(\theta) \right)}{\sqrt{1 - (D + C \sin(\theta))^2} - \left[ \left( \frac{B \cos(i) \sin(\theta)}{Q} - \frac{A \cos(\theta)}{Q} - B \sin(\theta) + C \cos(\theta) \right)^2 \left( \frac{(D + C \sin(\theta))}{(1 - (D + C \sin(\theta))^2)^{3/2}} \right) \right]} \quad (D-2)$$

where  $A = \cos(\psi) \sin(L_T + \frac{\theta}{Q})$

$B = \cos(\psi) \cos(L_T + \frac{\theta}{Q})$

$C = \cos(\psi) \sin(L_T + \frac{\theta}{Q}) \cos(i) + \sin(\psi) \sin(i)$ , and

$D = \cos(\psi) \cos(L_T + \frac{\theta}{Q}) \cos(\theta)$ .





## APPENDIX E: MINIMUM VALUES OF ANGULAR DISTANCE

The following tables will summarize minimum values of angular distance occurring at time  $t$ , and anomaly  $\theta$  for targets at different latitudes. They also contain probabilities of detection using the lateral range curves as equations (4-2) and (4-3), and provide the average probability of detection in a sidereal day.

Pass	Anomaly	Time (min)	CPA( $\lambda_{\min}$ ) (radian)	Probability $l_1(x)$	Probability $l_2(x)$
1	2.72	38.9	0.7723	0	0
2	9.24	132.0	0.4235	0	0
3	15.75	225.0	0.0909	0.787	1
4	22.12	316.0	0.3033	0	0
5	28.60	408.6	0.6589	0	0
6	35.26	503.6	0.9798	0	0
7	42.52	607.4	1.1328	0	0
8	49.65	709.3	0.9315	0	0
9	56.26	803.7	0.6009	0	0
10	62.74	896.2	0.243	0	0
11	69.21	988.7	0.1298	0.761	1
12	75.62	1080.2	0.4831	0	0
13	82.16	1173.6	0.8272	0	0
14	89.05	1272.0	1.0965	0	0
15	96.46	1377.9	1.0638	0	0
Average of probability of detection				0.103	0.133

Table E-1 Target's Latitude at 0°

Pass	Anomaly	Time (min)	CPA( $\lambda_{\min}$ ) (radian)	Probability $l_1(x)$	Probability $l_2(x)$
1	2.43	34.7	0.6118	0	0
2	8.98	128.2	0.3046	0	0
3	15.52	221.7	0.0916	0.786	1
4	21.85	312.2	0.3943	0	0
5	28.27	403.8	0.758	0	0
6	34.75	496.4	1.1212	0	0
7	42.90	612.8	1.3885	0	0
8	50.12	716.0	1.0612	0	0
9	56.58	808.2	0.6971	0	0
10	63.00	899.9	0.3342	0	0
11	69.41	991.5	0.0213	0.835	1
12	75.88	1083.9	0.3591	0	0
13	82.45	1177.8	0.6567	0	0
14	89.25	1274.9	0.8507	0	0
15	96.21	1374.4	0.8305	0	0
Average of probability of detection				0.108	0.133

Table E-2 Target's Latitude at 15°

Pass	Anomaly	Time (min)	CPA( $\lambda_{\min}$ ) (radian)	Probability $l_1(x)$	Probability $l_2(x)$
1	2.21	31.6	0.4205	0	0
2	8.76	125.2	0.1678	0.737	1
3	15.22	217.5	0.1398	0.755	1
4	21.57	308.1	0.4607	0	0
5	27.90	398.6	0.798	0	0
6	34.13	487.6	1.1363	0	0
7	39.90	570.0	1.4344	0	0
8	44.75	639.3	1.3944	0	0
9	50.67	723.8	1.0806	0	0
10	56.93	813.2	0.7414	0	0
11	63.26	903.7	0.4053	0	0
12	69.60	994.3	0.0987	0.782	1
13	76.11	1087.2	0.2133	0.000	0
14	82.67	1180.9	0.4554	0.000	0
15	89.34	1276.3	0.5962	0.000	0
16	96.08	1372.5	0.5825	0.000	0
Average of probability of detection				0.142	0.1875

Table E-3 Target's Latitude at 30°

Pass	Anomaly	Time (min)	CPA( $\lambda_{\min}$ ) (radian)	Probability $I_1(x)$	Probability $I_2(x)$
1	1.9999	28.6	0.1434	0.752	1
2	8.3457	119.2	0.1031	0.779	1
3	14.8421	212.0	0.2575	0.000	0
4	21.183	302.6	0.5044	0.000	0
5	27.4322	391.9	0.7543	0.000	0
6	33.5499	479.3	0.978	0.000	0
7	39.4697	563.8	1.1191	0.000	0
8	45.2789	646.8	1.1048	0.000	0
9	51.2332	731.9	0.9444	0.000	0
10	57.3778	819.6	0.7135	0.000	0
11	63.6431	909.1	0.4624	0.000	0
12	69.9807	999.8	0.2183	0.000	0
13	76.3183	1090.2	0.0836	0.792	1
14	82.8619	1183.7	0.1659	0.738	1
15	89.4144	1277.3	0.2531	0.000	0
16	95.9715	1370.9	0.2448	0.000	0
Average of probability of detection				0.191	0.25

Table E-4 Target's Latitude at 50°

Pass	Anomaly	Time (min)	CPA( $\lambda_{\min}$ ) (radian)	Probability $I_1(x)$	Probability $I_2(x)$
1	2.01	28.7	0.1077	0.776	1
2	8.30	118.6	0.1124	0.773	1
3	14.76	210.8	0.2857	0.000	0
4	21.09	301.2	0.5069	0.000	0
5	27.33	390.3	0.7282	0.000	0
6	33.45	477.8	0.9201	0.000	0
7	39.43	563.2	1.0351	0.000	0
8	45.34	647.6	1.0238	0.000	0
9	51.34	733.4	0.8919	0.000	0
10	57.48	821.2	0.6924	0.000	0
11	63.74	910.5	0.4694	0.000	0
12	70.07	1000.9	0.2504	0.000	0
13	76.40	1091.3	0.0939	0.785	1
14	82.86	1183.6	0.1133	0.772	1
15	89.41	1277.3	0.1682	0.737	1
16	95.97	1370.9	0.1602	0.742	1
Average of probability of detection				0.286	0.375

Table E-5 Target's Latitude at 55°

Pass	Anomaly	Time (min)	CPA( $\lambda_{\min}$ ) (radian)	Probability $I_1(x)$	Probability $I_2(x)$
1	1.92	27.5	0.1063	0.777	1
2	8.23	117.5	0.1801	0.000	0
3	14.60	208.6	0.3329	0.000	0
4	20.91	298.7	0.503	0.000	0
5	27.15	387.8	0.6691	0.000	0
6	33.30	475.7	0.8058	0.000	0
7	39.37	562.4	0.8824	0.000	0
8	45.41	648.7	0.875	0.000	0
9	51.50	735.6	0.7863	0.000	0
10	57.66	823.7	0.6427	0.000	0
11	63.91	913.0	0.4743	0.000	0
12	70.22	1003.1	0.3056	0.000	0
13	76.57	1093.8	0.1586	0.743	1
14	83.01	1185.8	0.0458	0.818	1
15	89.46	1277.9	0.012	0.841	1
16	95.92	1370.2	0.0065	0.845	1
Average of probability of detection				0.251	0.3125

Table E-6 Target's Latitude at 64°

Pass	Anomaly	Time (min)	CPA( $\lambda_{\min}$ ) (radian)	Probability $I_1(x)$	Probability $I_2(x)$
1	1.90	27.1	0.1052	0.777	1
2	8.22	117.4	0.1902	0.000	0
3	14.59	208.4	0.3378	0.000	0
4	20.89	298.4	0.5019	0.000	0
5	27.13	387.5	0.6617	0.000	0
6	33.28	475.5	0.7925	0.000	0
7	39.37	562.3	0.8653	0.000	0
8	45.42	648.8	0.8584	0.000	0
9	51.51	735.9	0.7739	0.000	0
10	57.68	824.0	0.6363	0.000	0
11	63.93	913.2	0.4743	0.000	0
12	70.24	1003.4	0.3115	0.000	0
13	76.59	1094.1	0.169	0.736	1
14	83.02	1186.0	0.0608	0.807	1
15	89.45	1277.8	0.0134	0.840	1
16	95.88	1369.7	0.0347	0.825	1
Average of probability of detection				0.249	0.3125

Table E-7 Target's Latitude at 65°

Pass	Anomaly	Time (min)	CPA( $\lambda_{\min}$ ) (radian)	Probability $l_1(x)$	Probability $l_2(x)$
1	1.80	25.7	0.15	0.748	1
2	8.15	116.4	0.2409	0.000	0
3	14.50	207.1	0.3615	0.000	0
4	20.80	297.1	0.4946	0.000	0
5	27.03	386.2	0.6224	0.000	0
6	33.21	474.5	0.7244	0.000	0
7	39.34	562.0	0.7799	0.000	0
8	45.45	649.3	0.7746	0.000	0
9	51.59	736.9	0.7101	0.000	0
10	57.78	825.3	0.6023	0.000	0
11	64.03	914.6	0.4723	0.000	0
12	70.32	1004.6	0.3401	0.000	0
13	76.67	1095.2	0.2232	0.000	0
14	83.03	1186.1	0.1408	0.754	1
15	89.41	1277.2	0.1142	0.771	1
16	95.73	1368.9	0.1159	0.770	1
Average of probability of detection				0.190	0.25

Table E-8 Target's Latitude at 70°

Pass	Anomaly	Time (min)	CPA( $\lambda_{\min}$ ) (radian)	Probability $l_1(x)$	Probability $l_2(x)$
1	1.72	24.5	0.2209	0	0
2	8.08	115.4	0.2914	0	0
3	14.41	205.9	0.3833	0	0
4	20.70	295.7	0.4842	0	0
5	26.95	384.9	0.5797	0	0
6	33.15	473.6	0.6544	0	0
7	39.32	561.7	0.6942	0	0
8	454.48	649.7	0.6905	0	0
9	51.66	737.9	0.644	0	0
10	57.87	826.6	0.5648	0	0
11	64.12	916.0	0.4674	0	0
12	70.42	1005.9	0.367	0	0
13	76.75	1096.3	0.2778	0	0
14	83.10	1187.1	0.212	0	0
15	89.48	1278.2	0.1782	0	0
16	95.86	1369.4	0.1817	0	0
Average of probability of detection				0	0

Table E-9 Target's Latitude at 75°

Pass	Anomaly	Time (min)	CPA( $\lambda_{\min}$ ) (radian)	Probability $l_1(x)$	Probability $l_2(x)$
1	1.68	24.0	0.2931	0	0
2	8.01	114.4	0.341	0	0
3	14.32	204.6	0.4032	0	0
4	20.61	294.4	0.4709	0	0
5	26.86	383.7	0.5342	0	0
6	33.09	472.7	0.5828	0	0
7	39.30	561.4	0.6084	0	0
8	45.51	650.1	0.606	0	0
9	51.72	738.8	0.5761	0	0
10	57.95	827.9	0.5244	0	0
11	64.22	923.1	0.4597	0	0
12	70.50	1007.1	0.3922	0	0
13	76.82	1097.3	0.3318	0	0
14	83.15	1187.8	0.287	0	0
15	89.50	1278.5	0.2641	0	0
16	95.85	1369.3	0.2662	0	0
Average of probability of detection				0	0

Table E-10 Target's Latitude at 80°

## LIST OF REFERENCES

- Bazaraa, Mokhtar S., Sherali, Hanif D., and Shetty C.M., *Nonlinear Programming Theory and Algorithms*, 2d ed., pp278-279, John Wiley & Sons, Inc., 1993.
- Clark, Rolf H., *Evaluating a Satellite Surveillance System*, Master's Thesis, Naval Postgraduate School, Monterey, California, October 1966.
- Colwell, Robert N. "Orbital Mechanics for Remote Sensing", *Manual of Remote Sensing* 2<sup>nd</sup> ed., vol.II, American Society of Photogrammetry, 1983.
- Friedman, Richard s., and others, *Advanced Technology Warfare*, Harmony Books, 1985.
- Larson, Wiley J. and Wertz, James R., *Space Mission Analysis and Design*, 2d ed., Microcosm, Inc., 1992.
- Naval Operations Analysis*, 2d ed. the United States Naval Institute, Annapolis, Maryland, 1989.
- Sellers, Jerry Jon, *Understanding Space An Introduction to Astronautics*, McGraw-Hill, Inc., 1994.
- Washburn, Alan R. "Earth Coverage by Satellites in Circular Orbit", paper presented at Department of Operations Research Naval Postgraduate School, Monterey, California, 1997.
- Washburn, Alan R. *Search and Detection* 3rd ed, The Institute for Operations Research and the Management Sciences, 1996.
- Wilkinson, C.K, "Coverage Regions: How They are Computed and Used," *Journal of the Astronautical Sciences*, Vol.42, No.1, pp.47-70, January-March 1994.
- Vallado, David A. *Fundamentals of Astrodynamics and Applications*, McGraw-Hill, Inc., 1997.





## INITIAL DISTRIBUTION LIST

1. Defense Technical Information Center ..... 2  
8725 John J. Kingman Road, Ste 0944  
Fort Belvoir, VA 22060-6218
  
2. Dudley Knox Library ..... 2  
Naval Postgraduate School  
411 Dyer Road  
Monterey, California 93943-5101
  
3. Office of the Naval Attache ..... 2  
Royal Thai Embassy  
1024 Wisconsin Ave, N.W.  
Washington DC. 20007
  
4. Professor J.N. Eagle (Code OR/ER) ..... 1  
Naval Postgraduate School  
Monterey, CA 93943
  
5. Professor Alan R. Washburn (Code OR/WS) ..... 1  
Naval Postgraduate School  
Monterey, CA 93943
  
6. Professor Supachai Sirayanone (Code MR/SY) ..... 2  
3100 Pleasant Circle  
Marina, CA. 93933
  
7. Institute of Advanced Naval Studies ..... 2  
105/3 Salaya-Taiyawas Rd.  
Salaya, Bhuthamolton  
Nakronprathom 73170 Thailand
  
8. LT Sarawoot Chiyangabut ..... 2  
15/102 Chokechaireummit  
Vibhavadii, Jatujake,  
Bangkok 10900 Thailand